Negative pion and muon fluxes in atmospheric cascades at a depth of 5 g cm^{-2}

M T Brunetti†, A Codino†, C Grimani†, M Menichelli†, M Miozza†,
I Salvatori, R L Golden‡, B L Kimbell‡, S A Stephens‡§, S J Stochaj‡,
W R Webber‡, F Massimo Brancaccio‖, P Papini‖, S Piccardi‖,
P Spillantini‖, G Basini¶, F Bongiorno¶, M Ricci¶, J F Ormes[+],
R E Streitmatter[+], M P De Pascale*, A Morselli* and P Picozza*

† Dipartimento di Fisica and INFN, Universita', Perugia, Italy
‡ New Mexico State University, Las Cruces, NM, USA
§ Tata Institute of Fundamental Research, Bombay, India
‖ Dipartimento di Fisica and INFN, Universita', Firenze, Italy
¶ INFN-Laboratori Nazionali di Frascati, Frascati, Rome, Italy
[+] Goddard Space Flight Center, Greenbelt, MD, USA
* Dipartimento di Fisica and INFN, Universita' Tor Vergata, Rome, Italy

Abstract. This paper reports observations of the absolute momentum differential fluxes of negative pions and muons between 4 and 15 GeV/c and between 0.3 and 15 GeV/c, respectively, at an atmospheric depth of 5 g cm^{-2}. The data have been collected by the balloon-borne experiment MASS (matter–antimatter space spectrometer) launched from Prince Albert (Canada) where the geomagnetic cut-off is 650 MV/c. The instrument was flown on the 5th of September 1989, the duration of the flight was 5.5 hours at an altitude of more than 117 000 ft. The measured fluxes are compared to calculations. The muon spectrum follows a power law in momentum with a spectral index of 2.36 above 2 GeV/c.

1. Introduction

The energy flux measurements of secondary particles, produced during the primary cosmic ray propagation in the atmosphere, allow a check of the atmospheric cascade calculations and the influence of the geomagnetic cut-off on the propagation process. In the energy range of this experiment, muons are generated mainly by the decay of pions produced in hadronic interactions in the atmosphere. Kaon decays become an important source of muons above 100 GeV (Gaisser 1990). Theoretical calculations have been carried out by several authors (for example, Badhwar *et al* 1977, Stephens 1981). Numerous measurements on the absolute muon spectra and charge ratio at sea level have been made in the past (Allkofer *et al* 1971, Ayre *et al* 1973, De Pascale *et al* 1993). We present the first negative pion and muon energy differential flux determination at float altitude. Preliminary results of this analysis have been reported earlier (Grimani *et al* 1993, Codino *et al* 1995). The final results presented in this paper have been obtained on the basis of an improved data analysis technique and efficiency determination. The event selection criteria and detector performance have been studied with pure samples of hadrons and electrons gathered during the flight. This method allows us to make an estimate with the precision limited only by

statistics and better than 1%, the selection efficiencies and the background of other particles on the muon and pion samples.

2. Instrument description

The MASS apparatus consisted of a time-of-flight scintillator system (TOF), a gas Cherenkov detector (G), a high resolution scintillator (S1), a superconducting magnet spectrometer and a streamer tube imaging calorimeter. The TOF system consisted of sixteen 1 cm thick paddles of plastic scintillator, Bicron 404. The paddles were arranged in four planes (T1–T2–T3–T4) of four paddles each. T1 and T2 were located at the top of the instrument and T3–T4 below the chambers of the magnetic spectrometer. The coincidence among the four planes of the TOF system generated the trigger for the apparatus. The G detector was filled with an equal gas mixture of Freon 12 and Freon 22 with a threshold Lorentz factor of 23 (Golden *et al* 1978, 1995). The Cherenkov light was collected by four mirrors, each mirror focusing the light on a RCA S83006E phototube. An onboard computer checked the scintillator S1 pulse-height. Only those events generating a signal greater than 0.25 times that corresponding to a minimum ionizing particle, were transmitted to the ground. The magnet spectrometer was comprised of a superconducting coil of NbTi and eight multi-wire proportional chambers (MWPC). The magnet generated a magnetic field ranging between 10 and 40 kG in the MWPC region while it was operated with a current of 120 A. The MWPC used a delay-line readout system. The maximum detectable rigidity was 118 GV/c. For a detailed description of the apparatus and, in particular, of the spectrometer performance see Golden *et al* (1991). The imaging calorimeter permitted the reconstruction of the topological structure of the particle interactions. It consisted of 40 layers of brass streamer tubes, 64 readout channels per plane, stacked in alternating x-view and y-view layers where the x-view is that along the magnet axis, and the y-view is parallel to the plane of the magnet. The total calorimeter thickness was of 7.3 radiation lengths and 0.75 nuclear interaction lengths (Basini *et al* 1988, Codino *et al* 1989). During the flight, the bottom part of the y-view was not working. Consequently, calorimeter selection criteria for data analysis have been applied to the x-view only.

3. Event selection

Float altitude negative muons and pions were selected among the bulk of negative charge particles, also consisting of electrons and antiprotons. Moreover, they have to be separated from upward moving albedo protons showing a negative curvature in the spectrometer.

3.1. Pion analysis

In order to separate negative pions from the electron background we used the particle interaction pattern in the calorimeter. It has to be noticed that the pion to electron ratio is about 0.04 between 4 and 15 GeV/c at 5 g cm^{-2} of atmospheric depth (Stephens 1981, Golden *et al* 1994). While electromagnetic cascades are collimated and generate many electron–positron pairs, secondary particles from hadronic interactions, in the energy range of this experiment, have low multiplicity and high opening angles. Out of the hadronic cascades we had to remove antiprotons and spill-over proton contamination. For this reason, we required a signal in the Cherenkov detector, limiting our analysis to the momentum range where pions are above the Cherenkov threshold and protons and antiprotons are well below. The Cherenkov threshold for pions was 3.2 GeV and for protons 21.6 GeV. In order to

Table 1. Negative pion selection criteria.

Test 1	At least five chambers in the direction of the maximum bending of the magnet (x-view) and three in the orthogonal direction (y-view) have good timing sums. Some combinations of bad chambers were rejected. For example, missing top or bottom chambers do not guarantee a reliable track reconstruction in the spectrometer.
Test 2	The least-squares fit to the reconstructed track must have $\chi_x^2 \leqslant 5$ and $\chi_y^2 \leqslant 7.5$.
Test 3	$0.4I_0 \leqslant Z_{T1} \leqslant 2I_0$ and $0.4I_0 \leqslant Z_{T2} \leqslant 2I_0$.
Test 4	Two or three planes show shower cluster.
Test 5	Cherenkov pulse height $\geqslant 1$ photoelectron.

avoid major contamination in the Cherenkov detector selection, we restricted our analysis to between 4 and 15 GeV/c. In this momentum interval the albedo proton flux amounts to less than 1% of the total proton flux (Dev Verma 1967). The contamination of albedo protons on the pion sample can be neglected since the TOF system allows their rejection. Pion selection criteria are summarized in table 1.

Tests 1 and 2 determine the reliability of the particle deflection determination in the magnetic spectrometer (Golden *et al* 1991).

Test 3 assures the selection of minimum ionizing particles, I_0 being the expected pulse-height generated by a minimum ionizing particle in the scintillators (De Pascale *et al* 1993). The above criteria allow the separation of negative, minimum ionizing particles from the total sample of events recorded during the flight.

In test 4 two or three shower clusters for particle interaction were required in the calorimeter. We have defined a shower cluster as a calorimeter plane where more than two wires, not necessarily contiguous, have been hit within five wires (corresponding to 2 Moliere radii) on either side of the particle trajectory. Particle tracks are extrapolated from the spectrometer down to the calorimeter bottom plane. A number of shower clusters greater than four above 4 GeV is characteristic of electromagnetic showers (Golden *et al* 1994), two or three shower clusters are generated by hadronic cascades and straight tracks (non-interacting particles) should not produce shower clusters, unless calorimeter noise simulates this kind of pattern. Even in this last case the overall topology of the interaction allows the particle identification.

In test 5 selected particles have been required to generate a signal in the Cherenkov detector corresponding to, at least, one photoelectron. The average number of photoelectrons produced by a fully relativistic particle was about ten. The selection criterion to determine if a signal was generated in the Cherenkov detector has been found by studying the distribution of the number of photoelectrons produced by particles with energies below and above the threshold.

Only pion events interacting in the calorimeter have been selected since pions penetrating the calorimeter without interaction are not distinguishable from negative muons. However, for flux determination the total number of pions has been considered, by estimating it from the number of interacting pions.

3.2. Muon analysis

The selection criteria for muons are reported in table 2.

Tests 1, 2 and 3 have been illustrated in the previous section.

Table 2. Negative muon selection criteria.

Test 1	At least five chambers in the direction of the maximum bending of the magnet (x-view) and three in the orthogonal direction (y-view) have good timing sums. Some combinations of bad chambers were rejected. For example, missing top or bottom chambers do not guarantee a reliable track reconstruction in the spectrometer.
Test 2	The least-squares fit to the reconstructed track must have $\chi_x^2 \leqslant 5$ and $\chi_y^2 \leqslant 7.5$.
Test 3	$0.4I_0 \leqslant Z_{T1} \leqslant 2I_0$ and $0.4I_0 \leqslant Z_{T2} \leqslant 2I_0$.
Test 4	Below 2 GeV/c. Cherenkov pulse-height < 1 photoelectron.
Test 5	Below 2 GeV/c, $\beta > 0.5$.
Test 6	Above 2 GeV/c. No more than one plane shows shower cluster. No more than 13 wire hits in the x-view of the calorimeter.

Tests 4 and 5 apply to particles in the momentum interval from 0.3 to 2 GeV/c. In this momentum range, only electrons are above the Cherenkov threshold. Thus, the absence of the Cherenkov detector signal is required for negative muon candidates (test 4). Low-energy albedo protons were removed from the candidate sample by requiring positive particle velocity (β) with the time-of-flight detector, characteristic of particles moving downward in the apparatus. With a TOF resolution of 250 ps and 227 cm separation, upward-moving particles were separated from down-moving particles by more than 25 standard deviations. In particular, it was required that β be greater than 0.5 (test 5). This criterion is not satisfied by protons below 1 GeV/c and was used because no albedo protons could pass the selection. Test 6 applies to muon candidates with momentum greater than 2 GeV/c when a straight track in the calorimeter is required. Test 6 gives a good separation among straight tracks and both hadronic and electromagnetic showers. Out of a sample of 300 electrons of energy > 2 GeV, no event was found with less than two shower clusters, or a number of total hit wires in the calorimeter x-view smaller than 15. By applying the cuts in test 6 to a sample of 300 interacting protons it has been found that two of them passed the cuts because of their first interaction point in the last few calorimeter planes. These kind of interactions generate one or even no shower clusters. Finally, out of 300 non-interacting protons just one did not pass the cuts because of calorimeter noise. No calorimeter cuts were used below 2 GeV/c. Electrons and hadrons below 1 GeV produce only a few secondary particles in the calorimeter, in this circumstance at those energies showers cannot be reliably separated from non-interacting particles. The limit of 2 GeV for the use of the calorimeter for particle separation includes no systematic error in the particle selection.

A sample of three interacting pions and 747 muons survived the selection criteria.

4. Geometrical factor and efficiencies

To determine the absolute pion and muon fluxes we had to estimate the geometrical factor, exposure time and efficiencies.

In order to study the particle interactions in the calorimeter, we have selected only those events fully contained in the apparatus down to the calorimeter bottom plane.

The geometric factor and chamber efficiency were found to be momentum dependent. The geometrical factor ranged from 77.65 cm^2 sr at 0.3 GV/c to 127.4 cm^2 sr above 3 GV/c. The error on the geometrical factor calculation is 0.1%. The efficiency of the tracking system
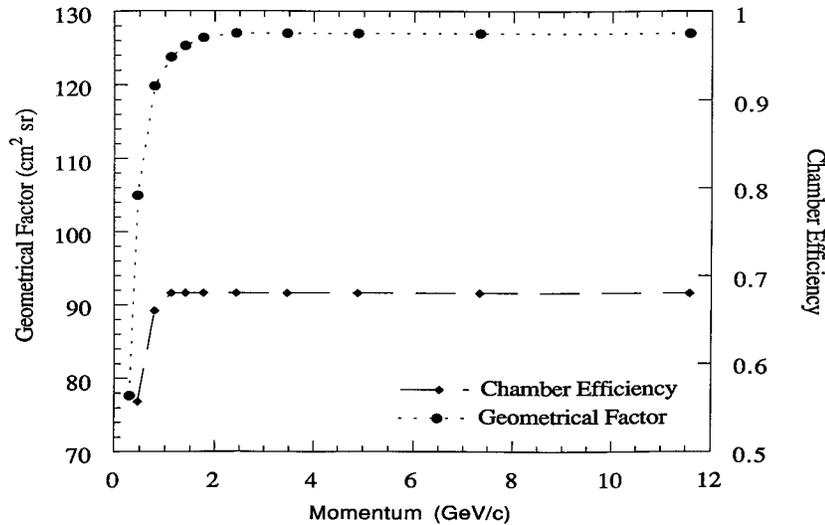
Figure 1. Experiment geometrical factor in cm^2 sr and chamber efficiency as a function of momentum.

was found constant above 1 GV/c and equal to 0.69 ± 0.01. In figure 1 we have shown both the geometrical factor and chamber efficiency versus momentum. The total experiment elapsed time was the difference between the occurrence of the first and the last collected event and it was equal to 19 812 s. A timer measured 33% dead time for data processing on board.

The scintillators had a response depending on the particle impact location for trigger generation resulting in an efficiency of 0.82 with an uncertainty of 0.01.

During the ground analogue tape recording of the data, 6% of events were lost since the disk write time of the ground computer system exceeded the buffering capability of the input interface.

The scintillator charge cut efficiency was 0.91 with a negligible uncertainty (De Pascale *et al* 1993). Landau fluctuations were mainly responsible for particles failing this test. The Cherenkov cut efficiency was 0.98 with negligible error (Golden *et al* 1994).

Pion cuts in the calorimeter were found to be a very powerful tool for separating these particles from both straight tracks and electromagnetic showers. The distributions of the number of shower clusters generated by particles non-interacting in the calorimeter and electromagnetic showers have been reported in figure 2.

Out of a sample of 94 muons and 143 electrons, above 4 GV/c, no particle passes test 4 for pions. Therefore, an upper limit at the 95% confidence level for the muon and electron contamination of 3.2% and 2.1%, respectively, on the pion sample is implied.

To verify that no pion events were lost with the calorimeter cuts, we released the calorimeter requirements. A visual scanning was performed to check that those events rejected by the calorimeter cuts did not show calorimeter interactions having low multiplicity and high opening angle secondaries.

To select muon events we have required for candidate events, with momentum smaller than 2 GeV/c, no Cherenkov light emission. During the first part of the flight, one of the Cherenkov phototubes was not working, for this reason we have restricted our analysis to the last 12 600 s of the flight.
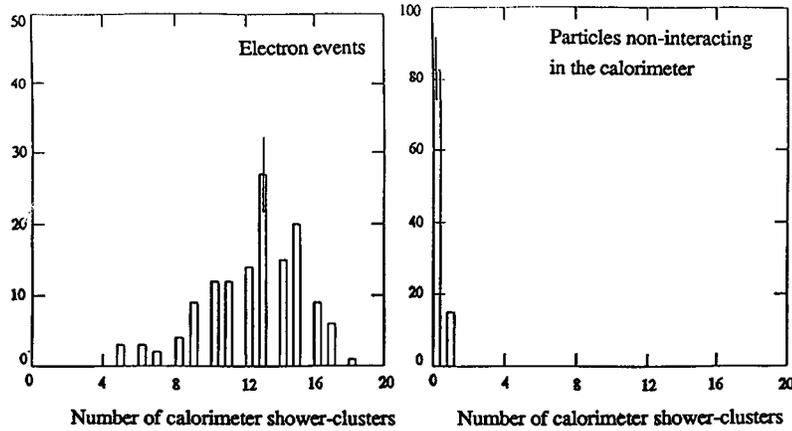
Figure 2. Distributions of the number of calorimeter shower clusters for electrons and non-interacting particles.

Table 3. Summary of muon observation.

Momentum interval (GeV/c)	Number of events	Geometrical factor (cm^2 sr)	Total efficiency	Flux (particles/(m^2 sr s GeV/c))
0.316–0.631	153	105	0.246	14.92 ± 1.30
0.631–1.00	150	120	0.292	9.21 ± 0.82
1.00–1.26	70	124	0.301	5.72 ± 0.72
1.26–1.58	64	125	0.305	4.16 ± 0.54
1.58–2.00	50	126	0.305	2.46 ± 0.36
2.00–3.00	119	126	0.324	1.47 ± 0.14
3.00–4.00	47	127	0.324	0.58 ± 0.09
4.00–6.00	47	127	0.324	0.29 ± 0.04
6.00–9.00	32	127	0.324	0.13 ± 0.02
9.00–15.0	15	127	0.324	0.031 ± 0.01

The TOF efficiency was 0.92. Inconsistencies in time measurements of counters T1, T2 or T3, T4 were responsible for the TOF inefficiency. As discussed in the 'event selection' section, above 2 GeV/c the calorimeter cuts did not determine loss of non-interacting particles for a fraction greater than 1% of the total sample. As a consequence, the calorimeter cut efficiency was assumed to be 1. It was also observed that a negligible interacting particle background passed the calorimeter cuts for muons. In table 3 the muon observations have been summarized. The total efficiency for muon selection reported in table 3 has been determined by multiplying individual selection and detector efficiencies.

5. Background contamination and flux corrections

In this section different sources of background contamination on the selected pion and muon samples are examined.

Albedo protons are removed by the TOF system requirements.

Using the spectrometer resolution functions (Golden *et al* 1991) it was possible to determine that high-energy protons (above 20 GV/c) have a probability of about 10^{-3}

to show a negative curvature in the rigidity range 2–20 GV/c. This probability rapidly vanishes for lower energy protons. These events are below the Cherenkov threshold and a fraction of them shows a hadronic interaction in the calorimeter. These particles present an error in deflection of greater than 1%. Therefore, it was possible to remove them. In addition, it has to be noted that for pion selection above 2 GeV/c a Cherenkov signal was required. Because the spill-over protons could pass the selection, a spurious signal from the detector had to be generated. The chance of accidental Cherenkov signals was found to be 5×10^{-4} (Golden *et al* 1995). Only half of these particles interact in the calorimeter between 2 and 20 GeV/c, and out of them only a fraction will produce the number of shower clusters required to pass the calorimeter selection. Therefore, any possible contamination of spill-over protons on the pion sample is well below 10^{-6}. On the basis of atmospheric antiproton calculations and galactic antiproton measurements (Stephens 1981, Stephens and Golden 1987) the contamination of these particles on the muon sample is 0.4%, also considering that only antiprotons not interacting in the calorimeter can be misidentified with muons. The antiproton to negative pion ratio is 0.10. The requirement of a Cherenkov signal removes the expected contamination due to antiprotons. By considering the rate of accidental Cherenkov signals the antiproton contamination goes down to 10^{-5} on the pion sample. Electrons passing the Cherenkov cut for low-energy muons, because of the detector inefficiency, have been subtracted. The convolution of the electron spectrum observed with the present experiment (Golden *et al* 1994) with the Cherenkov efficiency, the number of background electrons has been determined. The percentage of the subtracted particles ranges from 1.5% at 0.300 GeV/c to 0.2% at 2 GeV/c. Finally, before calculating the muon flux, we estimated and subtracted the background contamination of non-interacting pions in the sample of selected events from theoretical calculations (Stephens 1981).

Pion contamination is estimated to be less than 1% below 1 GeV smoothly increasing up to 13% at 15 GeV. In the muon flux measurement we have subtracted the expected pion background.

6. Results and discussion

To calculate the pion flux, the total number of pions can be determined by correcting the number of interacting pions by the probability of interaction in the calorimeter. This probability has been determined by using the inelastic cross section on deuterium and scaling it to a target having the same atomic number of the calorimeter (Gaisser 1990). We have found that 39% of pion events interact in the calorimeter. The corresponding total number of pions is 7.7. The pion flux between 4 and 15 GeV/c was found to be 0.0086 ± 0.0050 particles/(m^2 sr s GeV/c). In the pion and muon flux error determination we have included the estimated uncertainties on the selection cut efficiencies due to statistical and systematic errors. By using different selection criteria and evaluating the changes in the corresponding efficiencies we obtained precise information on the systematic errors. We have found that the main contribution to the flux error is due to statistical uncertainties. In figure 3 the pion and muon energy fluxes measured by this experiment have been reported and compared to calculations (Stephens 1981). The muon spectral index above 2 GeV/c is 2.36. There is good agreement between measured and calculated fluxes. Preliminary results on the determination of negative muon fluxes at deeper atmospheric depths with the MASS experiment have been reported in another paper (Circella *et al* 1993). These measurements can be used to check the calculations on atmospheric cosmic ray cascades and, in particular, the atmospheric neutrino flux (Gaisser *et*
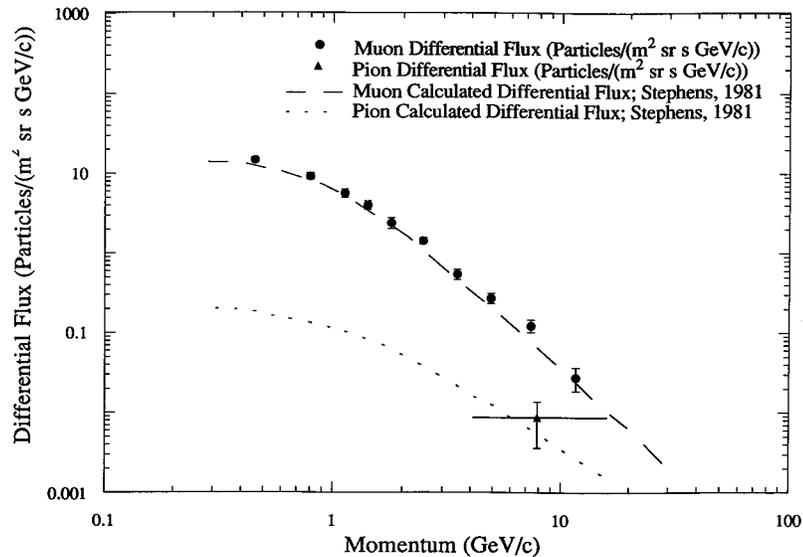
Figure 3. Measured and calculated negative pion and muon fluxes as a function of momentum. A power-law spectrum to the muon data gives a spectral index of 2.36 above 2 GeV/c.

al 1988). Data from longer flights are needed in order to reduce the measurement statistical errors.

Acknowledgments

References

Allkofer O C, Carstensen K and Dau W D 1971 The absolute cosmic ray muon spectrum at sea level *Phys. Lett.* **36B** 425–8
Ayre C A, Baxendale J M, Daniel B J, Hume C J, Nandi B C, Thompson M G, Whalley M R and Wolfendale A W 1973 The absolute muon spectrum in the range 3.5–700 GeV/c in the near vertical direction *Conf. Paper 13th Int. Cosmic Ray Conf.* pp 1754–63
Badhwar G D, Stephens S A and Golden R L 1977 Analytic representation of the proton–proton and proton–nucleus cross sections and its application to the sea-level spectrum and charge ratio of muons *Phys. Rev.* D **15** 820–31
Basini G *et al* 1988 A calorimeter coupled with a magnetic spectrometer for the detection of primary cosmic antiprotons *Nuovo Cimento* C **11** 339–51
Circella M *et al* 1993 Cosmic ray muon spectrum in the atmosphere *Conf. Paper 23rd Int. Cosmic Ray Conf.* **4** 503–7
Codino A *et al* 1989 Simulation of low-energy antiproton interactions in a sampling calorimeter *Nuovo Cimento* B **103** 319–31
Codino A *et al* 1995 Negative muon spectrum at 5 g cm^{-2} *Conf. Paper Vulcano Workshop* (*Nuovo Cimento* to appear)
De Pascale M P *et al* 1993 Absolute spectrum and charge ratio of cosmic ray muons in the energy region from 0.2 GeV to 100 GeV at 600 m above sea level *J. Geophys. Res.* **98** 3501–7

Dev Verma S 1967 Measurement of the charged and re-entrant albedo of the cosmic radiation *J. Geophys. Res.* **72** 915–25

Gaisser T K 1990 *Cosmic Rays and Particle Physics* (Cambridge: Cambridge University Press)

Gaisser T K, Stanev T and Barr G 1988 Cosmic ray neutrinos in the atmosphere *Phys. Rev.* D **38** 85–95

Golden R L, Badhwar G D, Lacy J L and Zipse J E 1978 A magnetic spectrometer for cosmic ray studies *Nucl. Instrum. Methods* **148** 179–85

Golden R L *et al* 1991 Performance of a balloon-borne magnet spectrometer for cosmic ray studies *Nucl. Instrum. Methods* A **306** 366–77

Golden R L *et al* 1994 Observations of cosmic ray electrons and positrons using an imaging calorimeter *Astrophys. J.* **436** 769–75

Golden R L *et al* 1995 Performance of a focused gas Cherenkov detector used for cosmic ray study *Nucl. Instrum. Methods* to be submitted

Grimani C *et al* 1993 Negative muon spectrum at 5 g cm^{-2} *Conf. Paper 23rd Int. Cosmic Ray Conf.* **4** 507–11

Stephens S A 1981 Secondary component of cosmic radiation at small atmospheric depths *Conf. Paper 17th Int. Cosmic Ray Conf.* **4** 282–6

Stephens S A and Golden R L 1981 The role of antiprotons in cosmic-ray physics *Space Sci. Rev.* **46** 31–91